

Semiempirical MO approach to the mechanism of the NIS-mediated nucleophilic addition to glycols: multicomponent intermediates as models to tackle reactivity in organic chemistry

Antonio J. Mota,^{a,*} Elena Castellanos,^b Luis Álvarez de Cienfuegos^{a,†} and Rafael Robles^a

^aDepartamento de Química Orgánica, Facultad de Ciencias, Universidad de Granada, Campus de Fuentenueva, 18071 Granada, Spain

^bInstituto de Química, Circuito Exterior, Ciudad Universitaria, Deleg. Coyoacán 04510, México, DF

Received 25 January 2005; accepted 9 March 2005

Abstract—A proposition for the nucleosidation mechanism of five-membered glycols promoted by *N*-iodo-succinimide (NIS), leading to 2'-deoxy-2'-iodo- β -nucleosides, is presented herein supported by semiempirical MO calculations. The proposed mechanism goes through the formation of multicomponent molecular intermediates that drastically diminish the total energy values when compared to charged intermediates (via iodonium species). The nucleosidation step was performed establishing either bicomponent (dihydrofuran–NIS) or tricomponent (dihydrofuran–NIS–silylated nucleobase) intermediates. The latter possibility has been shown to be the most likely (according also to DFT calculations), and suggests that the mechanism should take place in a concerted fashion. According to the tricomponent pathway, we have studied the stereoselectivity of the process, finding that the activation energy for the β -nucleosidation step is between ~ 6 kcal/mol (AM1) and ~ 10 kcal/mol (PM3) more favorable than that of the corresponding α -anomer, in agreement with the experimental results. The final step consists in an intramolecular silyl-transfer process accompanied by the NIS cleavage (in a different way depending on the calculation method employed), giving rise to the ultimate formation of *N*-silyl-succinimide.

© 2005 Elsevier Ltd. All rights reserved.

1. Introduction

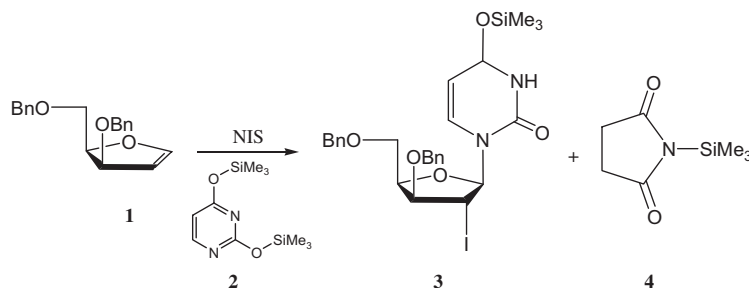
Nucleophilic addition to a double bond constitutes one of the most important organic reactions. This kind of process usually needs the presence of promoters activating the π -cloud. Particularly in carbohydrate chemistry, the nucleophilic addition over glycols, catalyzed by I^+ sources such as NIS¹ or sym-collidine iodonium perchlorate,² is of great interest. For instance, this approach has been widely employed in the case of glycosidations, even giving rise to oligosaccharides through a successive glycol-glycosyl acceptor coupling,³ and also in the synthesis of valuable 2-deoxy sugars.⁴ A concise revision about new applications of NIS shows noteworthy potential and great perspectives for this reagent.⁵

NIS-mediated nucleosidation reactions using five-membered glycols were initially carried out by Kim and Misco,⁶ and applied some years after by our group on sugar glycols (obtaining 2'-deoxy-2'-iodo- β -nucleosides with high stereoselectivity),⁷ and also on exocyclic sugar glycols (obtaining β -nucleoside-like derivatives along with open-chain nucleosides, depending on the nucleobase employed, also with high stereoselectivity).⁸ Another new NIS-mediated procedure for the selective obtaining of β -nucleosides has also been recently reported by our group.⁹ Motivated by these results, we decided to tackle the study of the most probable mechanism for these reactions based on theoretical calculations.

Semiempirical MO methods suffer certain well-known problems, such as the description of the hydrogen bond (especially problematic in MNDO), the description of typical organic hypervalent atoms (i.e., S or P), transition metals, transition states, or molecules that contain atoms for which a good parameterization does not exist, or simply, these parameters are not available.¹⁰ Nevertheless, these methods can quickly offer qualitative information about the atomic organization and electronic distribution of experimentally studied systems.

* Corresponding author at present address: Laboratoire de Chimie Quantique et de Modélisation Moléculaire, Institut Le Bel, Université Louis Pasteur, 4, rue Blaise Pascal, 67000 Strasbourg, France. Tel.: +33 3 90 241227; fax: +33 3 90 241589; e-mail: mota@quantix.u-strasbg.fr

† Present address: Massachusetts Institute of Technology, Department of Chemistry, Lab. Professor A. Klivanov, room 56-570, 77 Massachusetts Avenue, Cambridge, MA 02139-4307, USA.



Scheme 1. Simplified global nucleosidation process.

For this reason, semiempirical methods have become very useful tools in current organic chemistry. In spite of the problems related to the use of these methods in theoretical calculations, they have been widely employed, even for transition state calculations.¹¹ Furthermore, AM1 has been shown to be quite consistent in the study of carbohydrates¹² and nucleosides¹³ compared to NMR and X-ray diffraction analysis,¹⁴ substances that are present throughout this work.

Hence, we herein report a semiempirical study of the full NIS-promoted mechanism of nucleosidation of five-membered glycols (Scheme 1)⁷ employing the AM1 and PM3 semiempirical methods implemented in the Hyperchem 7.5 package.¹⁵ This study was performed by the means of multicomponent intermediates as convenient models accounting for the particular behavior of NIS.

To study this mechanism, we first used 2,3-dihydrofuran (DHF hereafter) as a model, in order to simplify the numerous calculations that had to be carried out. The stereoselectivity of the process, however, has been adequately explained using the glycal experimentally studied, namely compound **1**, once the whole mechanism was elucidated. The nucleobase employed in all calculations was *O,O'*-bis(trimethylsilyl)uracil **2**, although the obtained results could be extended to the other pyrimidinic bases and even to other nucleophiles. The proposed mechanism should be able to answer two important questions deriving from the experimental results:

- Why is the succinimide addition¹⁶ not observed to compete with the nucleobase, and even being an energetically more favorable process?
- Why does the addition of the nucleobase lead to β -nucleosides in a highly stereoselective way?

The mechanism has been divided into two main blocks: firstly, the nucleosidation step characterized by the generation of a tricomponent nucleoside-complex, and second, the termination step characterized by an intramolecular silyl transfer along with the NIS cleavage, affording the final products **3** and **4** (Scheme 1). Finally, it is noteworthy that the complete regioselectivity experimentally achieved for the nucleosidation process (the iodine atom always bonds C(3) and the nucleophile moiety C(2), referred to the DHF molecule) is only a consequence of the particular charge distribution in the oxygen-assisted double bond (Fig. 1).

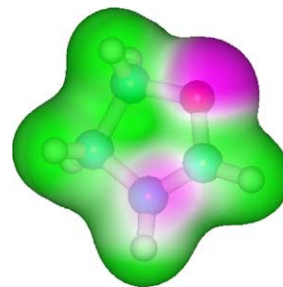


Figure 1. RHF-PM3 electrostatic potential representation for 2,3-dihydrofuran (DHF). Darker zones correspond to negative EP values.

2. Results and discussion

2.1. NIS cleavage. Formation of an oxocarbenium ion

It is generally accepted that NIS (and other iodonium-source compounds) acts by means of a liberated I^+ species that would interact with the double bond, leading to a cationic cyclic intermediate through the establishment of a π -complex.¹⁷ Nevertheless, it has not been possible to find a stable cyclic-iodonium (DHF- I^+) transition state although the I^+ species was directly placed at the C(3) position of the DHF molecule, with the system becoming the much more stable oxocarbenium ion (favored by 25–30 kcal/mol). Kim et al.^{2a} suggested the possibility of the existence of a hypothetical equilibrium between both ionic forms (cyclic iodonium-oxocarbenium), although according to these calculations, the cyclic state would not be established at all in this particular case (Table 1). In any case, the formation of the DHF-iodonium complex is a very favored process with respect to the separate components (DHF + iodonium). The problem is not establishing a cationic intermediate, but avoiding the counterion, which must also be considered in the evaluation of the total energy. Since the experimental reaction took place in dichloromethane as solvent, a hypothetical stabilization of both the

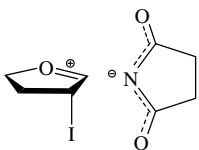
Table 1. The formation of the DHF- I^+ complex (values in kcal/mol)

System	AM1	PM3
DHF + Iodonium	0	0
DHF-iodonium complex	-121.63	-84.09



succinimide anion and the iodonium complex by the solvent should not acquire great importance. Thus, when taking into consideration all the species involved in the NIS cleavage, the total energy became very unfavorable (Table 2). This fact is related with the high energetic requirements to keep out two opposite charges. Note that a system of separate charges as the former would collapse leading to the corresponding nucleoside-like succinimide derivative, by attack of the succinimide anion to the C(2) position of the DHF molecule, currently positively charged. In fact, this process is highly favored and was experimentally observed in the absence of the corresponding nucleobase (Table 3).

Table 2. DHF-iodonium/succinimide anion system (values in kcal/mol)

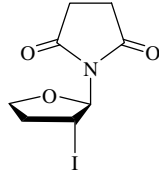


System	AM1	PM3
DHF + NIS	0	0
A + succinimide anion ^a	+129.26	+144.83

A = DHF-iodonium complex.

^a For this species a UHF calculation was done.

Table 3. The succinimide addition (RHF values in kcal/mol)



System	AM1	PM3
DHF + NIS	0	0
DHF-succinimide	-33.46	-20.83
Without/with charge separation difference	-162.72	-165.66

These results led us to consider that the reaction probably did not begin with NIS breaking, but through another way without charge separation. One attractive alternative has then been studied by considering the formation of multicomponent molecular complexes as intermediates and transition states. For simplicity, these intermediates could be roughly considered as charge transfer-like complexes.¹⁸ Requirements for this model are the existence of mobile π -electrons, the presence of hypervalent atoms, or low-energy unoccupied orbitals admitting lone electron pairs (and vice versa). It is predictable that the greater the number of units in the molecular complex, the better the stabilization energy for the whole system, due to a better effectiveness in the charge dispersion.

2.2. Bicomponent molecular-complex model

Bicomponent complex **5** is formed by the interaction between the iodine in NIS and the double bond in DHF

(Fig. 2). The formation of this complex avoids the possible nucleophilic attack on C(2) by the succinimide since NIS maintains its molecular unity (thus, there will be no free succinimide).

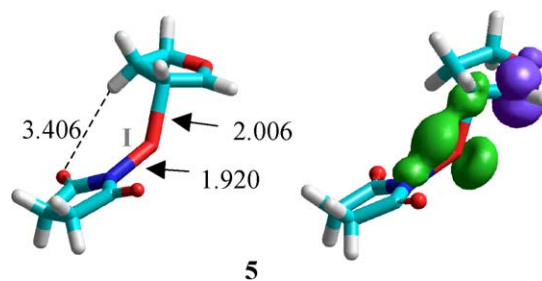


Figure 2. DHF-NIS bicomponent intermediate **5** (UHF-PM3). I = iodine atom. Distances shown are in angstrom.

Despite the distances shown for C(3)-I and I-N bonds (that seem to be normal σ -bonds), bond orders for C(3)-I and I-N are 0.60 and 0.49, respectively. Moreover, the current bond order for the C(2)-C(3) bond is 1.07 (as expected after the π -rearrangement). Note that the geometry of this complex (Table 4) is an intermediate between that of DHF and that of the DHF-iodonium complex.

Table 4. Some geometrical parameters for DHF-NIS and DHF-iodonium intermediates: d for distance (Å) and A for angle ($^\circ$)

System	Parameters ^a	PM3
DHF	$d[\text{O}(1)-\text{C}(2)]$	1.380
	$d[\text{C}(2)-\text{C}(3)]$	1.345
DHF-NIS complex	$d[\text{O}(1)-\text{C}(2)]$	1.358
	$d[\text{C}(2)-\text{C}(3)]$	1.466
	$d[\text{C}(3)-\text{I}]$	2.007
	$A[\text{C}(2)-\text{C}(3)-\text{I}]$	106.3
DHF-iodonium	$d[\text{O}(1)-\text{C}(2)]$	1.281
	$d[\text{C}(2)-\text{C}(3)]$	1.477
	$d[\text{C}(3)-\text{I}]$	2.010
	$A[\text{C}(2)-\text{C}(3)-\text{I}]$	108.4

^a d stands for distance and A for angle.

Complex **5**, however, is placed high in energy (~ 22 kcal/mol according to PM3) with respect to the separate DHF and NIS compounds, and can only be obtained when an unrestricted HF-PM3 calculation is performed. This leads to a structure with a diradical character, with the unpaired electrons essentially located onto C(2) and the iodine atom. A spin density representation for this structure can also be seen in Figure 2. Moreover, AM1 was not able to optimize its geometry within the convergence limits that we established for these complexes (see computational details), probably due to the fact that the potential well is actually very small for this species. All these features make the formation of this complex some unlikely, but we shall profit that PM3 allows to calculate it and we shall go to the end in order to compare the results obtained to the next model. Thus, from this bicomponent intermediate it was possible to obtain some important information.

For instance, the approximation of the silylated nucleobase generates a pre-associative tricomponent complex (left in Fig. 3) when the approximation angle φ (with respect to the DHF plane) lies at about 60° and the C(2)–N_{Nucl} distance is 3.423 Å (being N_{Nucl} the incoming nitrogen atom of the nucleobase). From this pre-associative complex, we established a transition state corresponding to the C(2)–N_{Nucl} bond formation (right in Fig. 3). At this moment, the energy roughly shows an important increase along with significant structural changes, the C(2)–N_{Nucl} distance and the φ angle being 1.997 Å and 77.7° , respectively (Table 5). The final point of the nucleobase approximation (Table 5, entry 6) corresponds to the formation of molecular complex of higher order **8** (Fig. 4). In this complex, the bond order

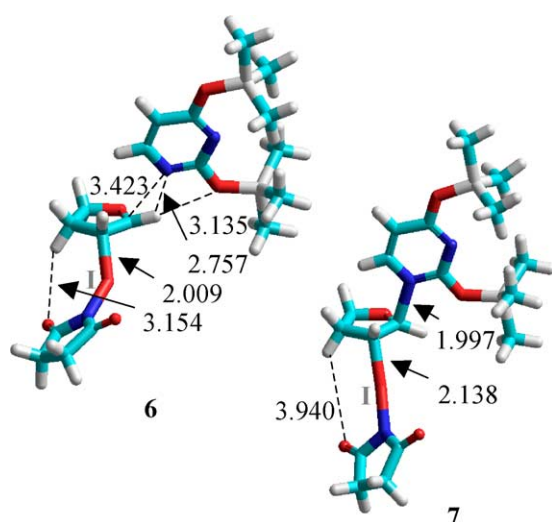


Figure 3. The pre-associative complex **6** (left), and the transition state **7** (right) for the bicomponent model. Distances shown are in angstrom.

Table 5. Structural parameters calculated for the nucleobase approximation (UHF–PM3)

Entry	$d[\text{N}-\text{C}(2)]$ (Å) ^a	φ (°)	$d[\text{C}(3)-\text{I}]$ (Å)	$D[\text{C}(5)-\text{O}-\text{C}(2)-\text{H}(2)]$ (°)	PM3 energy (kcal/mol)
1	∞	—	2.007	–165.89	0
2	4.993	60.2	2.008	–163.97	–0.09
3	3.423	60.7	2.009	–162.13	–0.37
4	3.003	73.8	2.005	–160.97	+1.93
5	1.997	77.7	2.138	+159.62	+8.52
6	1.547	— ^b	2.044	+126.71	+0.64

^a d stands for distance and D for dihedral angle.

^b The ring is no longer planar.

of the C(2)–N_{Nucl} bond is 0.83, therefore near to the single bond. However, as for complex **5**, the C(3)–I–N_{Succ} bonds seem to be a three center-two electron system, with bond orders of 0.50 for the C(3)–I bond and 0.42 for the I–N_{Succ} bond. This fact constitutes a typical behavior of hypervalent molecules.¹⁹

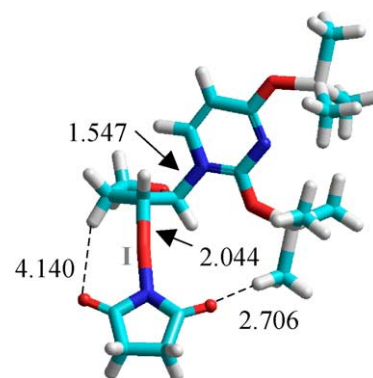


Figure 4. The PM3 tricomponent nucleoside-complex **8**. Distances shown are in angstrom.

The formation of the tricomponent nucleoside-complex **8** can be considered as the end of the nucleosidation step, since the C(2)–N_{Nucl} bond is already established. We can summarize the key species found throughout the bicomponent molecular-complex model in Table 6.

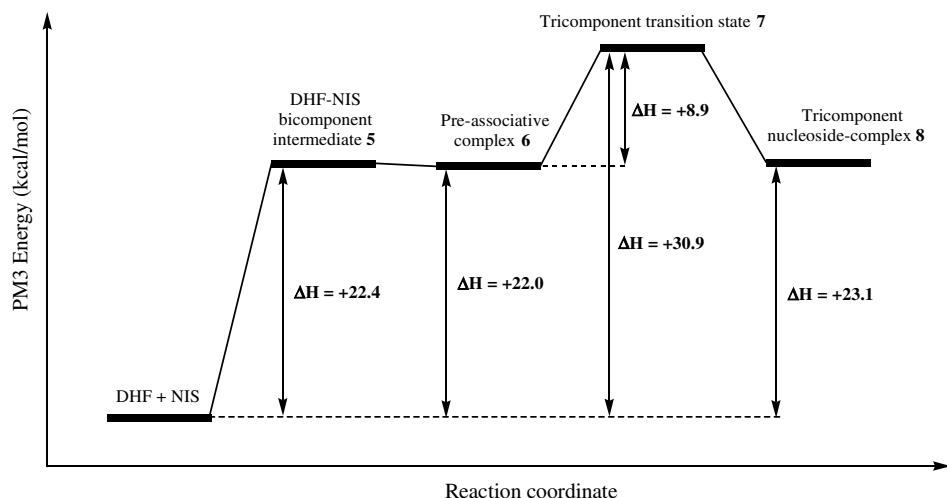
Table 6. PM3 energy in kcal/mol of the significant species found in the bicomponent complex model

System	PM3 energy
DHF + NIS + uracil ^a	0
Bicomponent complex 5	+22.4
Pre-associative complex 6	+22.0
Tricomponent transition state 7	+30.9
Tricomponent nucleoside-complex 8	+23.1

^a Uracil means *O,O'*-bis(trimethylsilyl)uracil **2** (Scheme 1).

Note that the energy difference between the transition state **7** and the bicomponent complex **5** is rather small (~ 9 kcal/mol). Nevertheless, the more important energetic cost corresponds to the first stage, namely the DHF–NIS complex formation **5**, which requires about 22 kcal/mol. Therefore, the transition state is finally located ~ 31 kcal/mol above the starting materials, a quite reasonable value indeed. Finally, the final tricomponent complex **8** has an energy value similar to that of the bicomponent complex, lying about 23 kcal/mol (Scheme 2).

Further calculations at the DFT level (B3LYP/6-31G*),²⁰ established that the bicomponent complex does not really exist (even as a diradical species), in agreement with the AM1 results that places NIS away from the double bond, existing only as a weak interaction between them. All this led us to establish a high-order complex discussed in the next section.



Scheme 2. Relative energies of the different intermediates obtained in the nucleosidation step: bicomponent molecular-complex model.

2.3. Tricomponent molecular-complex model

Conversely to the previous model, the tricomponent nucleoside-complex (Fig. 4) could be established in a single step. This means that DHF, NIS, and the silylated base, could simultaneously react in order to establish a high-order complex. This model has several important advantages: (a) intermediates can be obtained with both the AM1 and PM3 semiempirical methods; (b) the intermediate involved leading to the tricomponent transition state is energetically much more favorable, and finally (c) this situation could imply that a simultaneous addition takes place, which in turn would justify the fact for which succinimide does not compete with the nucleobase in the nucleosidation step at any moment.

In this model, the nucleosidation step can be divided in three stages:

- The formation of an early tricomponent intermediate, where DHF, NIS, and the silylated base establish a pre-associative complex before the formation of the transition state.
- The tricomponent transition state, where a simultaneous addition of NIS and the silylated base occurs.
- The formation of the already mentioned tricomponent nucleoside-complex.

These stages have been carefully studied by the AM1 and PM3 methods.

2.3.1. AM1 early tricomponent intermediate. Intermediate **9** is based on weak attractive electrostatic interactions along with Van der Waals interactions,²¹ predominating one of those mainly in function of the nucleobase approximation angle (φ) to the C(2) position in DHF. Thus, for this complex, a systematic study of some structural parameters was accomplished in function of φ , going from 35° to 90°, by 5° step. From the analysis of several parameter variations, an optimized geometry could be established for the early tricomponent intermediate **9** (Fig. 5).

Thus, when changing the φ value, the O(1)C(2)C(3)H(3) dihedral angle variation presents a saddle point for $\varphi \sim 65^\circ$ [values going far from 180° indicate the weakening of the bonding interaction between NIS and C(3)], and the C(2)–N_{Nucl} distance becomes minimum for φ values between 60° and 65°, which are the same angle values for which the C(3)–I distance presents an inflection (Table 7). In addition, from the variation of the charge on C(3) it can be concluded that the optimal interaction with the iodine atom is established between 55° and 75° (for which the higher negative values are obtained). Therefore, according to the AM1 calculations, we can set the most probable approximation angle at $\sim 65^\circ$ (Fig. 5). For this value, the associated energy is only 5.5 kcal/mol above the separate parent compounds. Note the high accessibility for this intermediate if we compare with the previous model.

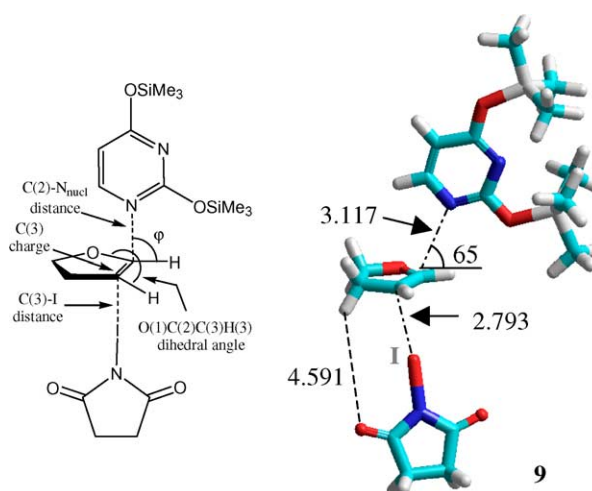
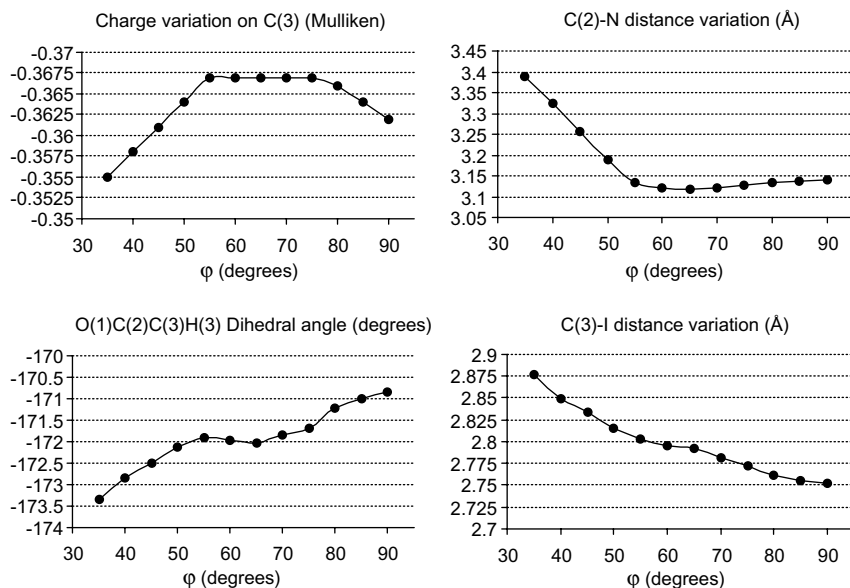


Figure 5. The optimal early tricomponent intermediate **9** according to AM1. Distances shown are in angstrom.

2.3.2. PM3 early tricomponent intermediate. Similar results were reached by PM3. Thus, the C(2) charge variation shows an optimal interaction between 70° and 80°.

Table 7. Parameter variations found on changing the φ angle value (RHF calculations using the 'eigenvector following' optimization algorithm)

φ (°)	AM1 energy (kcal/mol)	$d[\text{C}(2)\text{-N}]$ (Å) ^a	$d[\text{C}(3)\text{-I}]$ (Å)	$q[\text{C}(2)]$ (Mulliken)	$q[\text{C}(3)]$ (Mulliken)	$q[\text{H}(2)]$ (Mulliken)	$D[\text{OC}(2)\text{C}(3)\text{H}(3)]$ (°)
35.0	0	3.390	2.877	+0.029	-0.355	+0.218	-173.34
40.0	+0.08	3.323	2.849	+0.034	-0.358	+0.217	-172.84
45.0	+0.19	3.255	2.834	+0.039	-0.361	+0.216	-172.51
50.0	+0.34	3.188	2.815	+0.046	-0.364	+0.214	-172.12
55.0	+0.50	3.135	2.803	+0.052	-0.367	+0.211	-171.91
60.0	+0.64	3.120	2.795	+0.055	-0.367	+0.208	-171.97
65.0	+0.88	3.117	2.793	+0.058	-0.367	+0.205	-172.03
70.0	+1.13	3.122	2.782	+0.060	-0.367	+0.202	-171.85
75.0	+1.39	3.128	2.772	+0.062	-0.367	+0.200	-171.69
80.0	+1.64	3.135	2.761	+0.064	-0.366	+0.198	-171.23
85.0	+1.86	3.138	2.756	+0.064	-0.364	+0.195	-171.00
90.0	+2.11	3.140	2.752	+0.064	-0.362	+0.193	-170.83

^a d stands for distance, q for charge and D for dihedral angle.

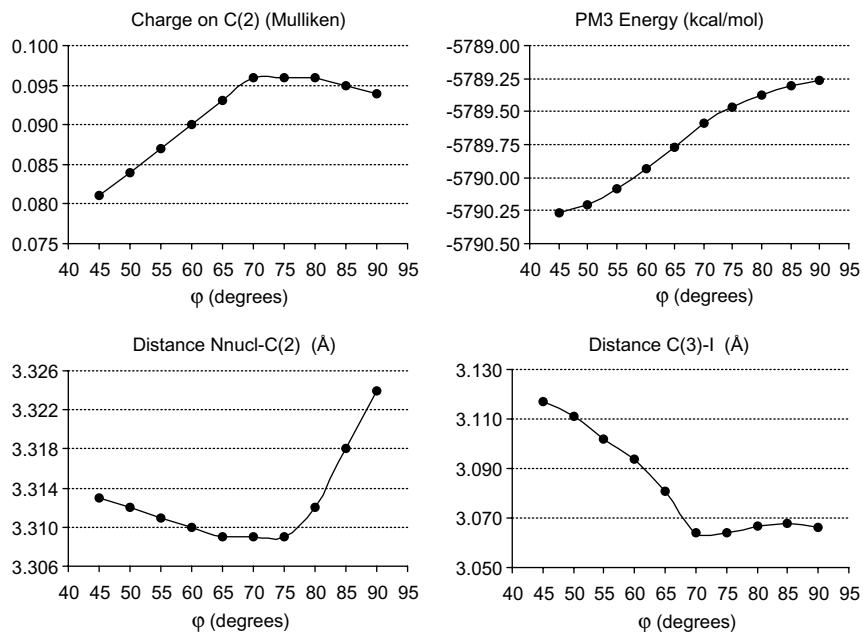
In addition, a minimum exists for the $\text{C}(2)\text{-N}_{\text{Nucl}}$ distance between 65° and 75° , and another one for the $\text{C}(3)\text{-I}$ distance between 70° and 75° (see Table 8 within supporting information). Hence, we presume that the optimal φ angle value is $\sim 70^\circ$ (Fig. 6), and the associated energy is only 4.8 kcal/mol above the separate components.

2.3.3. Affording the tricomponent nucleoside-complex. From the early tricomponent intermediate, a transition state (**10**) can be established where the two bonds [$\text{C}(2)\text{-N}_{\text{Nucl}}$ and $\text{C}(3)\text{-I}$] would form simultaneously. Unlike the previous model (where a sequential mechanism takes place), this fact leads to the idea that a concerted nucleosidation mechanism can occur. Thus, even though this transition state is formally the same than that obtained in the bicomponent model (according to PM3),²² the way to obtain it, is completely dissimilar. This transition state can be seen in Figure 7.

The final approximation of both NIS and the nucleobase leads to the key-step intermediate, namely the inter-

esting tricomponent nucleoside-complex already described in the case of PM3 (see Fig. 4 and related explanation in the text). With regards to AM1 (Fig. 8), for this complex the bond order for the $\text{C}(2)\text{-N}_{\text{Nucl}}$ bond is 0.78, which means that the bond is almost formed. As before, $\text{C}(3)\text{-I-N}_{\text{Succ}}$ bonds seem to be a three center-two electron system with bond orders of 0.53 for the $\text{C}(3)\text{-I}$ bond and 0.35 for the I-N_{Succ} bond. Relative energies for all the species implicated in the nucleosidation step according to the tricomponent model are shown in Table 9.

As can be seen, AM1 offers the most favorable energy values; for instance, ~ 25 kcal/mol are necessary in order to reach the transition state. However, a major difference is established for the energy of the tricomponent nucleoside-complex. Thus, PM3 calculations place this complex ~ 23 kcal/mol above the starting materials, whereas AM1 only estimates ~ 13 kcal/mol. This significant difference led us to carry out DFT calculations in order to establish a proper order of energy for the key-step nucleoside-complex **8**, finding that this tricomponent complex actually exists and AM1 gives the most

Table 8. Parameter variations found on changing the ϕ angle value (RHF calculations using the 'eigenvector following' optimization algorithm)

ϕ (°)	PM3 energy (kcal/mol)	$d[\text{N}-\text{C}(2)]$ (Å) ^a	$d[\text{I}-\text{C}(3)]$ (Å)	$q[\text{C}(2)]$ (Mulliken)	$q[\text{C}(3)]$ (Mulliken)	$q[\text{H}(2)]$ (Mulliken)	$D[\text{OC}(2)\text{C}(3)\text{H}(3)]$ (°)
45.0	0	3.313	3.117	0.081	-0.355	0.164	-174.14
50.0	+0.06	3.312	3.111	0.084	-0.355	0.161	-174.06
55.0	+0.19	3.311	3.102	0.087	-0.354	0.157	-173.81
60.0	+0.34	3.310	3.094	0.090	-0.354	0.154	-173.61
65.0	+0.50	3.309	3.081	0.093	-0.354	0.151	-173.28
70.0	+0.68	3.309	3.064	0.096	-0.354	0.148	-172.95
75.0	+0.80	3.309	3.064	0.096	-0.352	0.145	-172.93
80.0	+0.90	3.312	3.067	0.096	-0.349	0.142	-172.86
85.0	+0.97	3.318	3.068	0.095	-0.346	0.140	-172.71
90.0	+1.01	3.324	3.066	0.094	-0.343	0.138	-172.58

^a d stands for distance, q for charge and D for dihedral angle.

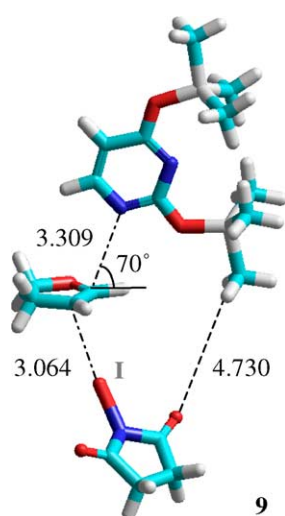


Figure 6. The optimal early tricomponent intermediate **9** according to PM3. Distances shown are in angstrom.

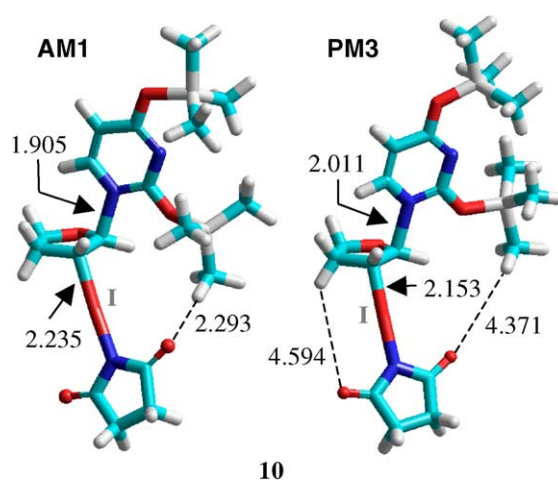


Figure 7. RHF AM1 (left) and PM3 (right) tricomponent transition states **10**. Distances shown are in angstrom.

accurate energy values and geometries.²³ The structural differences observed between the AM1 and DFT geom-

etries are a direct consequence of the almost planar description that the AM1 method systematically does over five-membered rings.²⁴

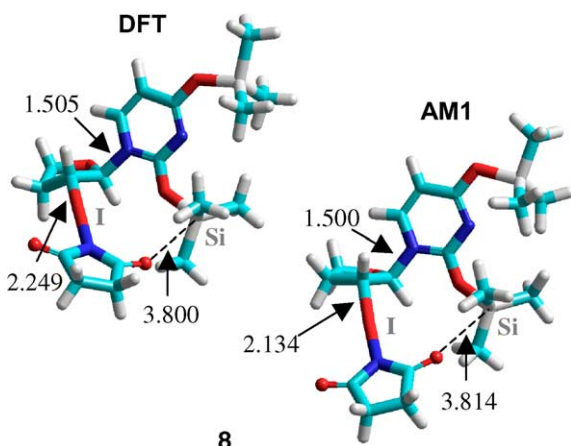


Figure 8. The DFT/6-31G* (left) and AM1 (right) tricomponent nucleoside complexes **8**. Distances shown are in angstrom.

Table 9. Energy values (kcal/mol) for the species implicated in the nucleosidation step in the tricomponent model

System	AM1	PM3	DFT/6-31G*
Isolated molecules ^a	0	0	0
Early complex 9	+5.5	+4.8	n.a. ^b
Tricomponent TS 10	+25.1	+29.4	+14.8
Nucleoside-complex 8	+13.0	+23.1	+8.1

^a DHF + NIS + *O,O'*-bis(trimethylsilyl)uracil.

^b This complex has not been calculated.

The complete pathway for this model is depicted in Scheme 3.

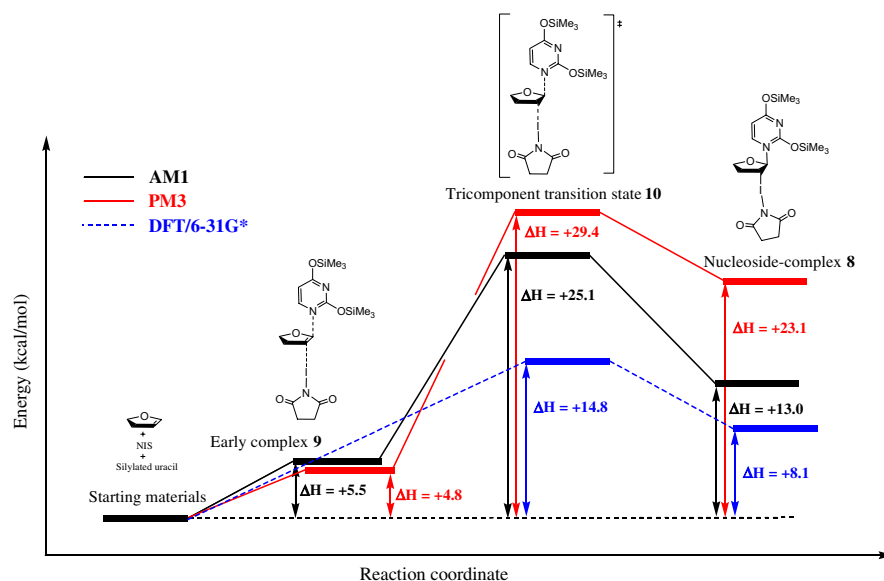
2.4. The silyl transfer

After the formation of the tricomponent nucleoside-complex **8**, the cleavage of the molecular complex takes place affording the final products (Fig. 1). This evolution probably goes through an intramolecular silyl transfer from the nucleobase to the NIS, which also promotes the NIS breaking affording the expected *N*-silyl-succini-

imide **4** along with the corresponding *trans*-2'-deoxy-2'-iodo-nucleoside (α or β stereochemistry has no sense in this case). In order to originate the transfer process, an adequate approximation of the NIS carbonyl group to the silicon atom of the nucleobase is necessary, the TMS group being transferred through an S_N1 -like mechanism. This was reached by slight structural changes with a very low energetic cost by means of an intermediate that we called 'close complex'. Moreover, it was possible to establish two different pathways that in turn depend on the method employed: one leading directly to the formation of **4** if we use PM3, and the other to the formation of first the isomeric *O*-silyl-succinimide if AM1 is employed. Since the latter compound is thermodynamically less stable than the *N*-silyl derivative, the reaction finally evolves toward **4** by a second intramolecular transfer of the TMS group.

2.4.1. AM1 silyl transfer. In the tricomponent nucleoside-complex **8**, the O_{NIS} -Si and Si- O_{Nucl} distances are 3.814 and 1.865 Å, respectively. From this complex, an intermediate can be established with the necessary structural requirements to provoke the silyl-transfer process between the nucleoside and one of the NIS oxygens (for which we called it oxygen pathway'). This intermediate ('close-complex' **11**) has an energetic cost of only ~5 kcal/mol, and now the mentioned O_{NIS} -Si and Si- O_{Nucl} distances are 2.671 and 1.881 Å, respectively. Note that an important approximation of the NIS oxygen to the silyl moiety has occurred (more than 1 Å).

It was surprising to find that the whole transfer reaction was obtained in one single RHF calculation from the 'close complex' without any energetic barrier, evolving directly toward the *O*-silyl intermediate **12** (Fig. 9). This fact allows us to capture several outstanding intermediate points that were collected stopping the same calculation job each time at a different number of optimization cycles (always starting at the same point: the close-complex intermediate **11**). From this data, it should be noted



Scheme 3. Pathway of the nucleosidation process in the tricomponent molecular-complex model.

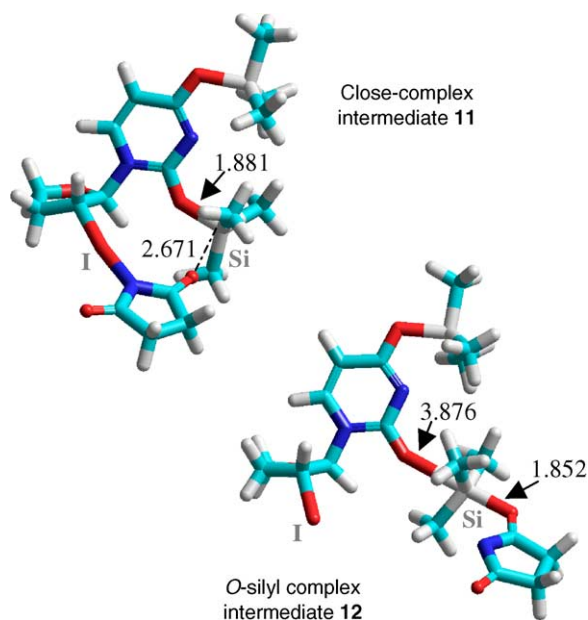
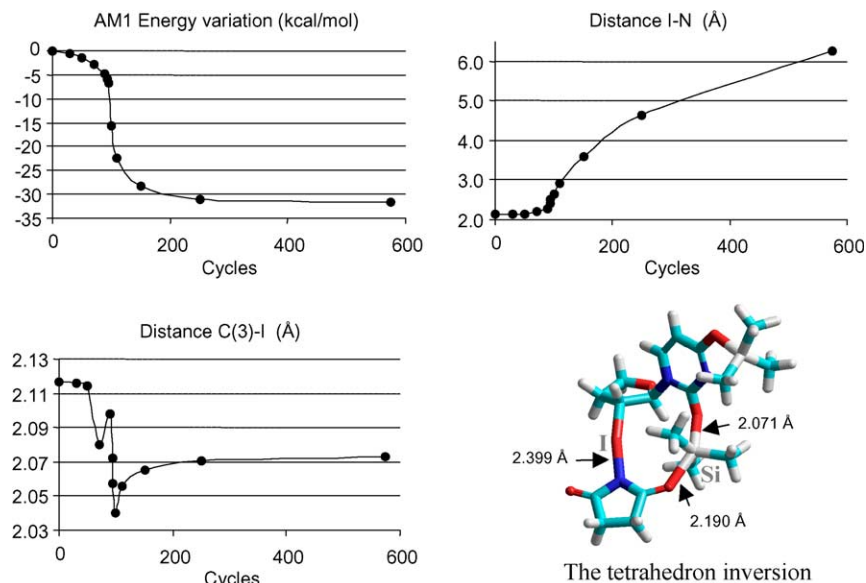


Figure 9. Starting **11** and ending **12** intermediates in the AM1 silyl-transfer process. Distances shown are in angstrom.

that NIS remains as a molecular unity until the $O \rightarrow O'$ silyl transfer occurs. This moment is characterized by a tetrahedron inversion on the silyl moiety: the N–I distance has changed from 2.120 to 2.399 Å, and in the neighborhood of this point a great irregularity for the C(3)–I and C(2)–N_{Nucl} distances is displayed (Table 10 and figures therein). From this moment, the I–N bond is definitely broken, leading to the final nucleoside-*O*-silyl-succinimide complex **12**. It should be noted that this tetrahedron inversion takes place with no energetic barrier, and then, it does not constitute a transition state (see the AM1 energy variation in Table 10). Finally, the nucleoside-*O*-silyl-succinimide complex **12** (Fig. 9) is readily converted in its *N*-silylated isomer owing to its greater stability. For this new intramolecular $O \rightarrow N$ silyl migration **13** the activation energy was found to be only 8.8 kcal/mol (Fig. 10).

On forcing the system to allow the nitrogen atom to approach the silyl group instead of the oxygen atom (and then performing the ‘nitrogen pathway’), the final obtained product is the nucleoside-*N*-silyl-succinimide **14** intermediate. However, the ‘nitrogen pathway’ needs

Table 10. Following the transfer of the TMS group through the ‘oxygen pathway’



Cycles ^a	AM1 energy (kcal/mol)	$d[C(2)-N_{Nucl}]$ (Å)	$d[C(3)-I]$ (Å)	$d(I-N_{NIS})$ (Å)	$d(O_{NIS}-Si)$ (Å)	$d(Si-O_{Nucl})$ (Å)
0	0	1.500	2.117	2.120	2.671	1.881
30	-0.63	1.487	2.116	2.125	2.703	1.886
50	-1.49	1.487	2.114	2.146	2.694	1.905
70	-2.75	1.474	2.080	2.204	2.276	2.057
90	-4.67	1.481	2.098	2.264	2.400	1.963
94	-5.77	1.471	2.072	2.399	2.190	2.071
95	-6.69	1.466	2.057	2.501	2.039	2.163
100	-15.76	1.467	2.040	2.655	1.862	2.362
110	-22.26	1.458	2.056	2.910	1.853	2.562
150	-28.14	1.461	2.065	3.590	1.868	2.672
250	-30.96	1.462	2.071	4.638	1.869	2.608
End	-31.76	1.462	2.073	6.256	1.867	2.603

^a Tracks: 0–40: soft accommodation of the succinimide moiety; 40–93: quick translation of the silyl moiety toward the oxygen atom of succinimide; 94–95: silicon tetrahedron inversion; 95–End: silyl transfer and breaking of NIS.

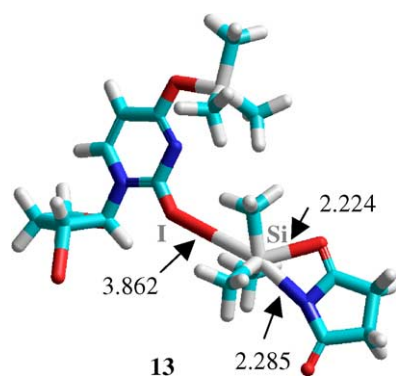


Figure 10. Transition state for the $O \rightarrow N$ silyl transfer in the final intermediate. Distances shown are in angstrom.

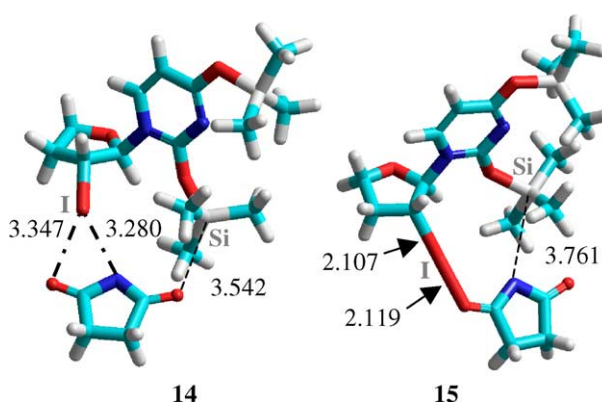


Figure 11. The transition state (left) that leads to the O-I intermediate in the 'nitrogen pathway' (right). Distances shown are in angstrom.

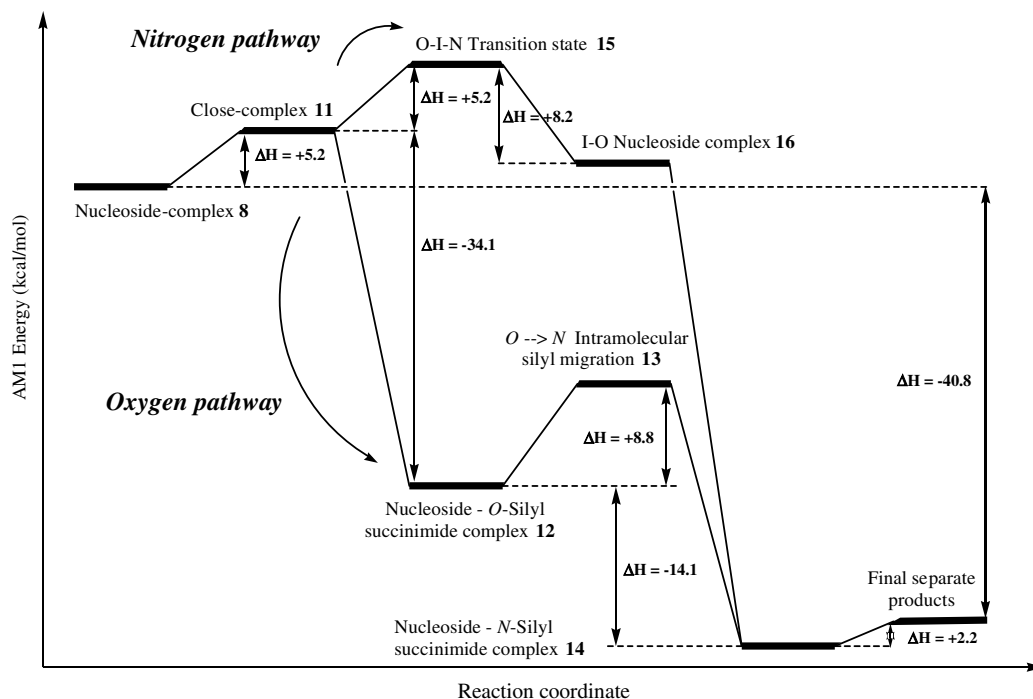
to create a new transition state **15** in order to obtain the necessary O-I intermediate **16** that adequately orientates

the nitrogen atom toward the silicon moiety that will be transferred (Fig. 11, Table 11). The complete silyl-transfer process (according to AM1) is depicted in Scheme 4, from which an unquestionable preference for the 'oxygen pathway' is granted by the AM1 semiempirical method.

Table 11. The nitrogen pathway

System	AM1 energy (kcal/mol)
Nucleoside-complex 8	0
Close-complex 11	+5.2
O-I-N transition state 15	+10.5
I-O complex 16	+2.3

2.4.2. PM3 silyl transfer. In the tricomponent nucleoside-complex **8**, the O_{NIS} -Si and Si- O_{Nucl} distances are 4.741 and 1.732 Å, respectively. In the same manner, a close-complex intermediate **11** can be established where these distances are, respectively, 3.988 and 1.736 Å, with an energetic cost of only ~ 0.3 kcal/mol. As far as both pathways are concerned, the results afforded by PM3 show a preference for the 'nitrogen pathway' against the 'oxygen pathway', although the energy differences between them are quite small. According to the PM3 calculations, the reaction always evolves through the I-O complex independently of the pathway followed. This means that it takes place first an intramolecular N-I \rightarrow O-I interchange in the NIS moiety, in order to allow a better approximation of the NIS nitrogen atom to the silyl group in the nucleobase (Fig. 12, Table 12). In addition, the final product always is *N*-silyl-succinimide independent of the pathway followed. This fact is not surprising in the case of the 'nitrogen pathway'. In the case of the 'oxygen pathway' a change of the forthcoming atom in the proximities of the tetrahedron inversion



Scheme 4. Nucleoside \rightarrow NIS silyl-transfer process according to AM1 following the 'oxygen' and 'nitrogen pathway'.

takes place, transforming the *O*-approaching in an *N*-approaching (Fig. 12).

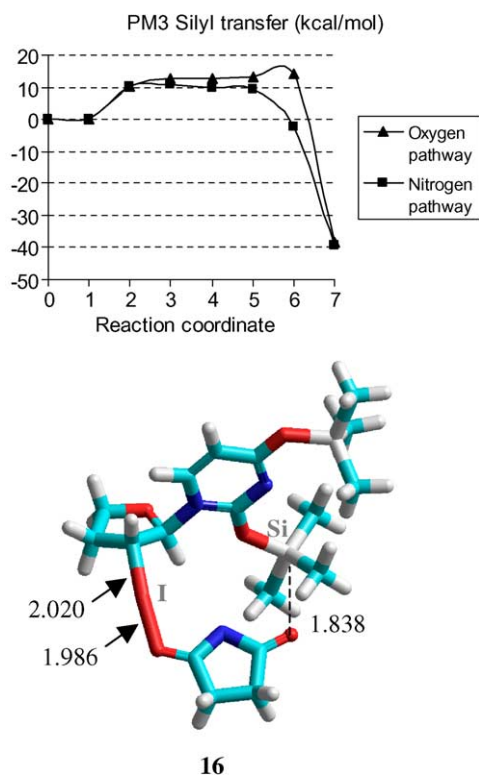


Figure 12. Above: PM3 ‘nitrogen’ and ‘oxygen pathways’. Points 0, 1, 2, and 7 in the reaction coordinate are common for both pathways and correspond to the nucleoside-complex **8**, the close-complex **11**, the I–O complex **16**, and the nucleoside-*N*-silyl succinimide complex **14**, respectively. Below: the I–O complex **16**. Distances shown are in angstrom.

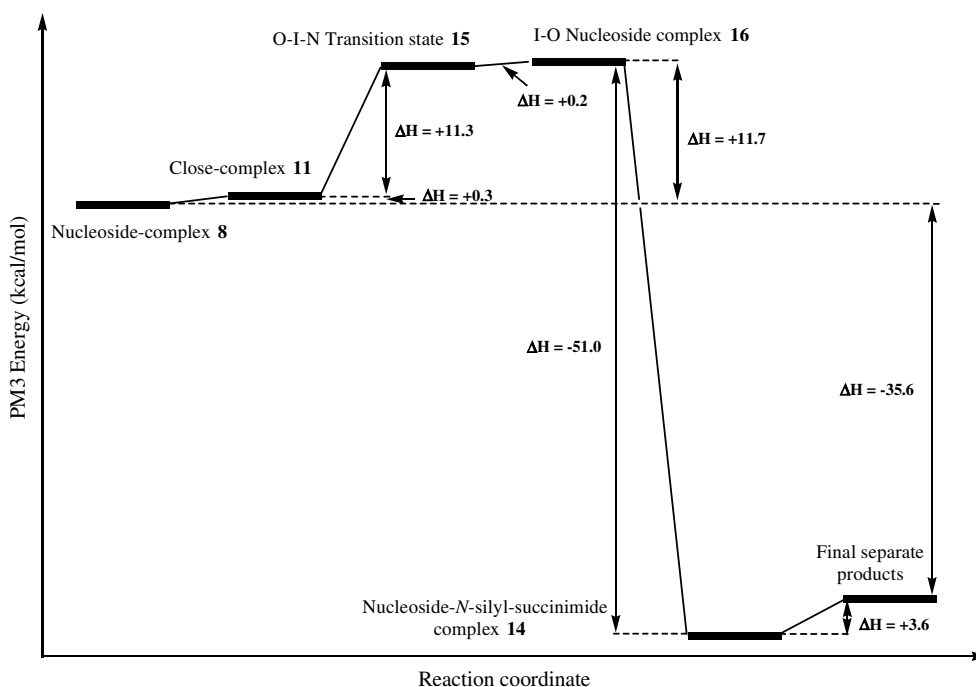
Table 12. The formation of the PM3 I–O complex

System	PM3 energy (kcal/mol)	$d(\text{O}_{\text{NIS}}-\text{Si})$ (Å)	$d(\text{Si}-\text{O}_{\text{Nucl}})$ (Å)
Nucleoside-complex 8	0	4.741	1.732
Close-complex 11	+0.3	3.924	1.733
O–I–N TS 15	+11.5	4.089	1.739
I–O complex 16	+11.7	4.220	1.734

From a mechanistic point of view, the ‘nitrogen pathway’ is similar in both methods. However, the ‘oxygen pathway’ is quite different. For instance, according to PM3, the I–N bond in the NIS moiety must be broken before the approximation to the silyl group (from the I–O complex). In addition, according to PM3 an O→N approximation interchange takes place in the proximities of the silicon atom. This fact implies that PM3 always prefers the production of **4**, independent of the pathway followed. Conversely, the AM1 method first produces the *O*-silyl-succinimide when the ‘oxygen pathway’ is considered. Another difference to be highlighted is that PM3 considers the evolution of the O–I–N intermediate toward the I–O complex as an almost isoenergetic process. However, the energetics of the whole silyl-transfer step is shown to be a much more favorable process according to the description of AM1. All this can be seen in Scheme 5, where the complete PM3 silyl-transfer step is shown.

2.5. The diastereoselectivity of the nucleosidation

Once the mechanism had been proposed, it seemed quite interesting to explore the predictable diastereoselectivity that this mechanism can afford from a qualitative point of view; thus, we have taken the same starting molecular



Scheme 5. Nucleoside→succinimide silyl transfer according to PM3.

system that was employed in the experimental work,⁷ namely the five-membered glycal **1** (Fig. 1). We began making a conformational search for compound **1**, doing three times 500 optimizations (molecular mechanics: Amber 99 force field). The non-repeated conformations were recalculated by the different semiempirical methods. Both AM1 and PM3 found three conformations within 1 kcal/mol, and a different geometry for the optimal conformation.²⁵ Therefore, the analysis was done in each case with a different conformer, respecting the obtained results from each method (Fig. 13).

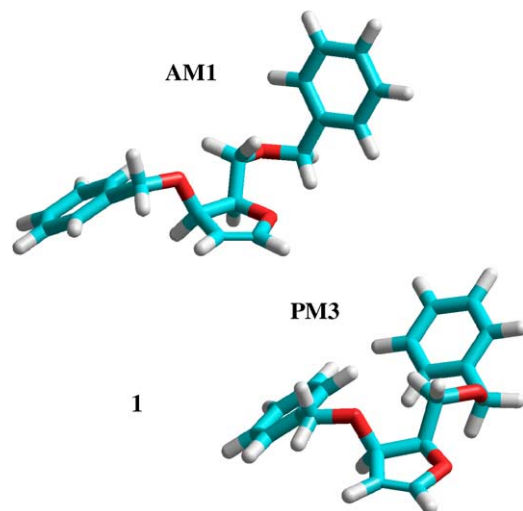


Figure 13. AM1 and PM3 lower-energy conformers.

A moderate distant interaction complex was found between NIS and the corresponding glycal, where NIS would be situated at 4.5 Å (AM1). At this distance, there is no difference between the energy of the α - and the β -NIS approximation. Furthermore, when NIS was situated ~ 1 Å closer, only slight differences in energy between the addition upon both faces appeared, showing the α -NIS approximation (then, β -nucleosidation) to be more stable (-1.2 kcal/mol for a C(3)–I distance of 3.26 Å). This means that the approximation of the bulky iodine to O(3) on the β face generates an increasing electronic repulsion due to the establishment of an all-*cis* derivative. Hence, it is quite acceptable to think that the substituent present at C(3) is the main responsible of the stereoselectivity, the steric effects predominating in order to avoid an all-*cis* configuration.²⁶

2.5.1. Bicomponent molecular complex. The geometry of the bicomponent complex is quite similar to that shown by this molecular intermediate when we used DHF as a structural model.

As before, AM1 is not able to properly establish the NIS-1 bicomponent molecular intermediate (in concordance, however, to DFT calculations). Anyhow, it can be seen that an all-*cis* complex (NIS approximation on the β -face) generates a more steric hindered intermediate (Fig. 14). In fact, the PM3 energy difference between the α -NIS and the β -NIS complex was found to be 3.3 kcal/

mol, the α -NIS isomer being the more stable. Obviously, this situation favors the β -nucleobase addition, but it seems a small value if we want to get a very high stereoselectivity.

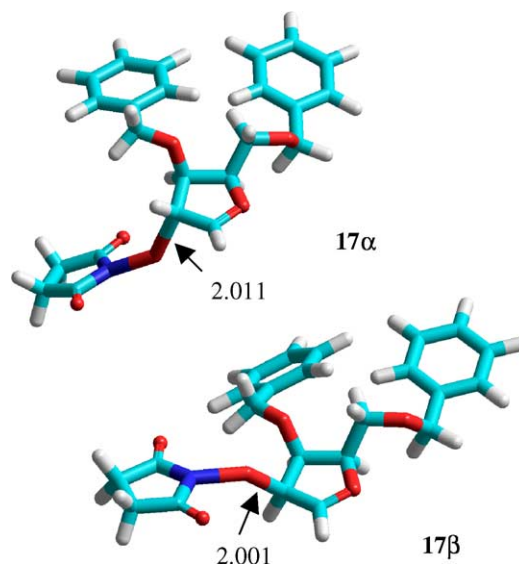


Figure 14. The α - and β -NIS-1 bicomponent complexes **17 α** and **17 β** . Distances shown are in angstrom.

2.5.2. Tricomponent molecular complex. Geometries of the tricomponent transition states **18** and nucleoside complexes **19** are quite similar compared to those found for the DHF model (Fig. 15). In the same way, they could be established by all the calculation methods employed.

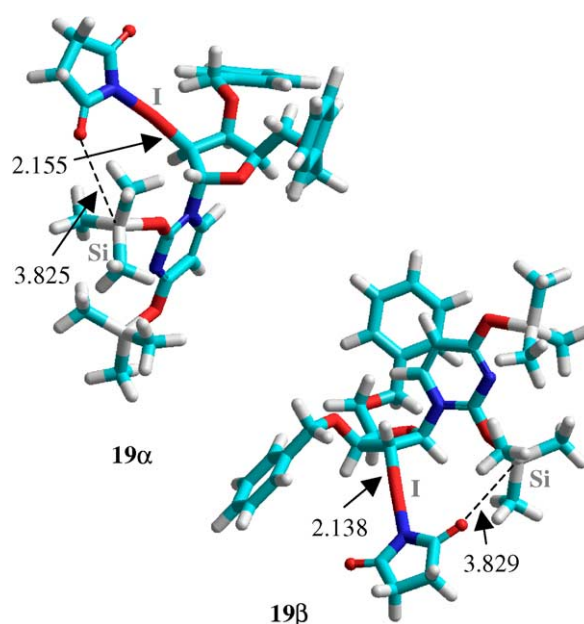


Figure 15. AM1 α -**19 α** and β -nucleoside-complex **19 β** . Distances shown are in angstrom.

Remarkably in this case, the energy differences between the α - and β -addition in the tricomponent complex

model became greater: ~ 6 kcal/mol according to AM1 and ~ 10 kcal/mol according to PM3. These values match better in order to explain the high stereoselectivity found experimentally. Energy differences between the α - and β -nucleosidation for transition states, nucleoside-complexes and final products are summarized in Table 13.

Table 13. Energy of the nucleoside-complex intermediate and final products

System	AM1	PM3
DiBnDHF + NIS + Uracil ^a	0	0
Transition state (β -nucleosidation)	+17.28	+27.26
Transition state (α -nucleosidation)	+22.87	+35.94
Diff. transition state β/α	-5.59	-8.68
Nucleoside-complex (β)	+5.65	+19.94
Nucleoside-complex (α)	+11.48	+29.92
Diff. intermediate β/α	-5.83	-9.98
Global β -nucleosidation	-34.14	-10.84
Global α -nucleosidation	-28.93	-3.20
Diff. nucleosidation β/α	-5.21	-7.64

^a Uracil means *O,O'*-bis(trimethylsilyl)uracil.

From this data it can be concluded that:

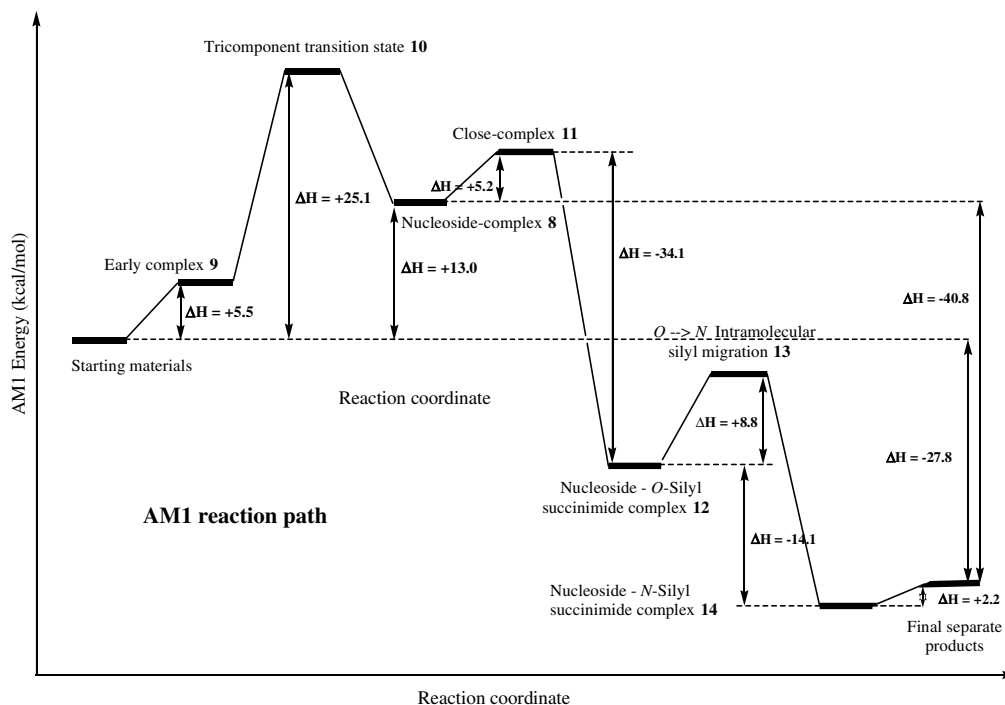
(a) The bicomponent model is not a suitable model for reproducing this mechanism, due mainly to three reasons: firstly, only PM3 can establish these complexes, AM1 being in concordance with DFT calculations. Secondly, the energies displayed for intermediates are much higher in this model. This conclusion has an important effect because this means that the mechanism is more likely concerted

through a tricomponent molecular-complex model. Finally, the tricomponent model can much better explain the high β -stereoselectivity for the nucleosidation process encountered experimentally, owing to the high energetic differences between the α - and β -nucleobase additions. These significant differences appear as a consequence of the hindrance showed in the formation of an 2,3,5-*cis* derivative. This points to the fact that these intermediates are actually the key step of the whole process.

- (b) The silyl transfer in the whole system takes place in the same manner that was shown before for the DHF model. AM1 again shows a preference for the formation of the *O*-silyl-succinimide complex, where a new intramolecular O \rightarrow N silyl transfer would finish the reaction. Nevertheless, PM3 prefers going directly to the *N*-silyl-succinimide complex.
- (c) The determining step consists of the nucleosidation step according to the AM1 calculations, whereas according to PM3, the determining step is the silyl-transfer process.
- (d) It seems that the AM1 semiempirical method reproduces quite well the whole process, displaying the smaller energies throughout the reaction path and establishing a valuable concordance with DFT test calculations. Thus, we can summarize the most probable complete reaction in Scheme 6.

3. Conclusions

In summary, we have carried out a semiempirical study of the mechanism for the NIS-mediated addition of silylated pyrimidinic bases to glycols (even though these



Scheme 6. AM1 reaction pathway of the whole tandem nucleosidation-silyl transfer reaction for DHF: tricomponent molecular complex model.

results could be extended to other nucleophiles) through the formation of multicomponent molecular complexes. The establishment of bicomponent intermediates was only reached by PM3. From these complexes, the tricomponent intermediates were obtained, which could be equally obtained from a direct mechanism through the formation of early tricomponent intermediates. The advantage is that the necessary energy to get the latter compounds is much smaller. This means that the addition took place in a simultaneous way, avoiding, in this manner, the possible addition of the succinimide moiety on C(2). The results disclosed herein emphasize the significance of the tricomponent species in the NIS-promoted reaction. From this point the termination reactions begins, namely NIS-breaking and silyl transfer (from the silylated base to NIS). According to AM1, it takes place first from the silyl-transfer process whereas PM3 first breaks the NIS molecule. In any case, the tricomponent nucleoside-complex seems to be the key step in the whole process because an easy intramolecular silyl transfer can then take place (uracil→NIS) along with the NIS breaking that would lead to the final products in a simple way with a low energetic cost. Thus, from AM1 we can propose a way that has no energetic barrier for the silyl-transfer process whereas according to PM3 an N–I→O–I transference (~11–12 kcal/mol) is necessary. The application of the proposed mechanism to the experimental target molecule showed a high preference for the β -nucleosidation (~6–10 kcal/mol), in agreement with the experimental results in terms of the high stereoselectivity found. We can rationalize this fact taking into account that the NIS approaching leading to an all-*cis* distribution produces greater steric repulsions. In addition, AM1 performs better for this particular case with regard to the DFT calculations carried out. This conclusion is also in agreement with the literature (see above).^{12–14}

4. Computational details

The computational study was performed by means of AM1 and PM3 semiempirical MO calculations, all methods implemented in the HyperchemTM 7.5 package.¹⁵ Calculations were carried out as close-shell type (RHF), unless otherwise was indicated, using the Polak–Ribiere optimization algorithm, except for transition states for which eigenvector-following algorithm was employed. Concerning geometries, convergence limits for the optimization process were fixed at 0.01 kcal $\text{\AA}^{-1} \text{mol}^{-1}$ (RMS gradient) for the stable compounds and 0.05 kcal $\text{\AA}^{-1} \text{mol}^{-1}$ (RMS gradient) for intermediates and transition states. The limit for the iterative SCF calculations was fixed at 0.001 kcal mol^{-1} . Transition states were evaluated with estimated initial geometries using the transition state research implemented in the HyperchemTM 7.5 package, by means of a trial-and-error sequence, and characterized by its unique negative frequency. Geometries for the five-membered glycal **1** (see Scheme 1) were obtained after a conformational searching, which were done using the Amber 99 force field. Then, the different conformers were recalculated by the different semiempirical methods

used. DFT calculations were carried out at the B3LYP level with the Gaussian 03 program²⁷ using the standard 6-31G* basis set for all atoms except for iodine, for which SDD basis set was used with an added polarization d function (exponent 0.266).²⁸

Acknowledgements

The authors would like to thank the Junta de Andalucía and the Universidad de Granada (Spain) for the provision funds and technical support for the development of this work.

References

- (a) Middleton, D. S.; Simpkins, N. S. *Synth. Commun.* **1989**, *19*, 21–29; (b) Lynch, M.-J.; Simpson, J.; Weavers, R. T. *Aust. J. Chem.* **1993**, *46*, 203–212; (c) Smietana, M.; Gouverneur, V.; Mioskowski, C. *Tetrahedron Lett.* **2000**, *41*, 193–195.
- (a) Kim, C. U.; Luh, B. Y.; Martin, J. C. *J. Org. Chem.* **1991**, *56*, 2642–2647; (b) Danishefsky, S. J.; Bilodeau, M. T. *Angew. Chem., Int. Ed. Engl.* **1996**, *35*, 1380–1419, and references cited therein.
- (a) Mootoo, D. R.; Konradsson, P.; Udodong, U.; Fraser-Reid, B. *J. Am. Chem. Soc.* **1988**, *110*, 5583–5584; (b) Friesen, R. W.; Danishefsky, S. J. *J. Am. Chem. Soc.* **1989**, *111*, 6656–6660; (c) Friesen, R. W.; Danishefsky, S. J. *Tetrahedron* **1990**, *46*, 103–112.
- (a) Thiem, J.; Karl, H.; Schwentner, J. *Synthesis* **1978**, 696–698; (b) Thiem, J.; Karl, H. *Tetrahedron Lett.* **1978**, *19*, 4999–5002; (c) Thiem, J.; Ossowowski, P. *J. Carbohyd. Chem.* **1984**, *3*, 287–313; (d) Thiem, J.; Prahst, A.; Wendt, T. *Liebigs Ann. Chem.* **1986**, 1044–1056; (e) Thiem, J.; Klaffke, W. *J. Org. Chem.* **1989**, *54*, 2006–2009; (f) Costantino, V.; Imperatore, C.; Fattorusso, E.; Mangoni, A. *Tetrahedron Lett.* **2000**, *41*, 9177–9180.
- Speicher, A.; Eicher, T. *J. Prakt. Chem.* **1998**, *340*, 278–280.
- Kim, C. U.; Misco, P. F. *Tetrahedron Lett.* **1992**, *33*, 5733–5736.
- Robles, R.; Rodríguez, C.; Izquierdo, I.; Plaza, M.-T.; Mota, A. *Tetrahedron: Asymmetry* **1997**, *8*, 2959–2965.
- Robles, R.; Izquierdo, I.; Rodríguez, C.; Plaza, M.-T.; Mota, A. J.; Álvarez de Cienfuegos, L. *Tetrahedron: Asymmetry* **2002**, *13*, 399–405.
- (a) Álvarez de Cienfuegos, L.; Rodríguez, C.; Mota, A. J.; Robles, R. *Org. Lett.* **2003**, *5*, 2743–2745; (b) Robles, R.; Rodríguez, C.; Álvarez de Cienfuegos, L.; Mota, A. J. *Tetrahedron: Asymmetry* **2004**, *15*, 831–838.
- (a) Foresman, J. B.; Frisch, A. E. *Exploring Chemistry with Electronic Structure Methods*, 2nd ed.; Gaussian: Pittsburgh, PA, USA, 1996; (b) Jensen, F. *Introduction to computational chemistry*; John Wiley & Sons Ltd: Chichester, England, 1999.
- Some examples: (a) McIver, J. W., Jr.; Komornicki, A. J. *Am. Chem. Soc.* **1972**, *94*, 2625–2633; (b) Wu, C. S.; Neely, W. C.; Worley, S. D. *J. Comput. Chem.* **1991**, *12*, 862–867; (c) Dory, Y. L.; Soucy, P.; Drouin, M.; Deslongchamps, P. *J. Am. Chem. Soc.* **1995**, *117*, 518–529; (d) Fabian, W. M. F.; Kollenz, G. *J. Chem. Soc., Perkin Trans. 2* **1995**, 515–518; (e) Parusel, A. B. J.; Schamschule, R.; Piorun, D.; Rechthaler, K.; Puchala, A.; Rasala, D.; Rotkiewicz, K.; Köhler, G. *J. Mol. Struct.* **1997**, *419*, 63–75; (f) Markovic, Z.; Konstantinovic, S.; Juranic, I.; Dosen-

- Micovic, L. *Gazz. Chim. Ital.* **1997**, *127*, 429–434; (g) Lorenc, L.; Pavlovich, V.; Juranich, I.; Mihailovich, M. L.; Bondarenko-Gheorghiu, L.; Krstich, N.; Dabovich, M. *Molecules* **1999**, *4*, 272–278; (h) Grotjahn, M.; Jäger, N.; Drexler, H.-J.; Holdt, H.-J.; Kleinpeter, E. *J. Mol. Model.* **1999**, *5*, 72–77; (i) Bohm, S.; Pohl, R.; Kuthan, J. *Collect. Czech. Chem. Commun.* **1999**, *64*, 1761–1769; (j) Merino, P.; Mates, J. A. *Arquivoc* **2001**, *xi*, 12–30; (k) Mota, A. J.; Robles, R.; Álvarez de Cienfuegos, L.; Lamencá, A. *Tetrahedron Lett.* **2004**, *45*, 3349–3353; (l) Álvarez de Cienfuegos, L.; Mota, A. J.; Rodríguez, C.; Robles, R. *Tetrahedron Lett.* **2005**, *46*, 469–473.
12. Hamann, C. H.; Koch, R.; Pleus, S. *J. Carbohydr. Chem.* **2002**, *21*, 53–63.
13. Santana, L.; Teijeira, M.; Uriarte, E.; Balzarini, J.; De Clercq, E. *Eur. J. Med. Chem.* **2002**, *37*, 755–760.
14. (a) Lai, T.; Marsh, R. E. *Acta Crystallogr.* **1973**, *1328*, 1982–1989; (b) Stolarski, R.; Pohorille, A.; Dudycz, L.; Shugar, D. *Biochim. Biophys. Acta* **1980**, *610*, 1–9; (c) Orozco, M.; Luis, C.; Mallol, J.; Canela, E. I.; Franco, R. *J. Pharm. Sci.* **1990**, *79*, 133–137; (d) Baumgartner, M. T.; Motura, M. I.; Contreras, R. H.; Pierini, A. B.; Briñón, M. C. *Nucleos. Nucleot. Nucleic Acids* **2003**, *22*, 45–62.
15. Hyperchem™, Hypercube, Inc., 1115 NW 4th Street, Gainesville, FL 32601, USA.
16. Sowa, C. E.; Kopf, J.; Thiem, J. *J. Chem. Soc., Chem. Commun.* **1995**, 211–212.
17. Dewar, M. J. S. In *Electronic Theory of Organic Chemistry*; Cumberlege, G., Ed.; Oxford University Press: London, 1949, Chapter VIII.
18. Morokuma, K. *Acc. Chem. Res.* **1977**, *10*, 295–300.
19. Albright, T. A.; Burdett, J. K.; Whangbo, M. H. *Orbital Interactions in Chemistry*; John Wiley & Sons Ltd: Baffins Lane, Chichester, 1985, Chapter 3.
20. (a) Becke, A. D. *Phys. Rev. A* **1988**, *38*, 3098–3100; (b) Lee, C.; Yang, W.; Parr, R. G. *Phys. Rev. B* **1988**, *37*, 785–789; (c) Becke, A. D. *J. Chem. Phys.* **1993**, *98*, 5648–5652.
21. Price, S. L. In *Molecular Interactions*; Scheiner, S., Ed.; John Wiley & Sons Ltd: Baffins Lane, Chichester, 1997, Chapter 9.
22. Slight differences can be found because in the bicomponent model, the starting product was the bicomponent intermediate, and the different intermediates were calculated on approaching the base moiety (Table 5). For the tricomponent model, a complete ‘unconstrained’ search for the transition state was found.
23. For instance, in the tricomponent nucleoside-complex **8**, the key C(2)–N_{Nucl} distance (Å) is 1.547 (PM3), **1.500** (AM1), and **1.509** (DFT). In the same manner, in the tricomponent transition state **10**, this distance becomes 2.011 (PM3), **1.905** (AM1), and **1.909** (DFT).
24. (a) Ferguson, D. M.; Gould, I. R.; Glauser, W. A.; Schroeder, S.; Kollman, P. A. *J. Comput. Chem.* **1992**, *13*, 525–532; (b) Giordan, M.; Custodio, R. *J. Comput. Chem.* **1996**, *17*, 156–166.
25. Due to the different treatments that AM1 and PM3 semiempirical methods grant to the phenyl groups’ interactions, differences in the optimal three-dimensional arrangement for these groups are usually found.
26. Burdett, J. *Steric Repulsion in Chemical Bonds: a Dialog*; John Wiley & Sons Ltd: Baffins Lane, Chichester, 1997.
27. Frisch, M. J.; Trucks, G. W.; Schlegel, H. B.; Scuseria, G. E.; Robb, M. A.; Cheeseman, J. R.; Montgomery, J. A., Jr.; Vreven, T.; Kudin, K. N.; Burant, J. C.; Millam, J. M.; Iyengar, S. S.; Tomasi, J.; Barone, V.; Mennucci, B.; Cossi, M.; Scalmani, G.; Rega, N.; Petersson, G. A.; Nakatsuji, H.; Hada, M.; Ehara, M.; Toyota, K.; Fukuda, R.; Hasegawa, J.; Ishida, M.; Nakajima, T.; Honda, Y.; Kitao, O.; Nakai, H.; Klene, M.; Li, X.; Knox, J. E.; Hratchian, H. P.; Cross, J. B.; Adamo, C.; Jaramillo, J.; Gomperts, R.; Stratmann, R. E.; Yazyev, O.; Austin, A. J.; Cammi, R.; Pomelli, C.; Ochterski, J. W.; Ayala, P. Y.; Morokuma, K.; Voth, G. A.; Salvador, P.; Dannenberg, J. J.; Zakrzewski, V. G.; Dapprich, S.; Daniels, A. D.; Strain, M. C.; Farkas, O.; Malick, D. K.; Rabuck, A. D.; Raghavachari, K.; Foresman, J. B.; Ortiz, J. V.; Cui, Q.; Baboul, A. G.; Clifford, S.; Cioslowski, J.; Stefanov, B. B.; Liu, G.; Liashenko, A.; Piskorz, P.; Komaromi, I.; Martin, R. L.; Fox, D. J.; Keith, T.; Al-Laham, M. A.; Peng, C. Y.; Nanayakkara, A.; Challacombe, M.; Gill, P. M. W.; Johnson, B.; Chen, W.; Wong, M. W.; Gonzalez, C.; Pople, J. A. *Gaussian 03, Revision B.02*; Gaussian: Pittsburgh, PA, 2003.
28. Energies and Cartesian coordinates are available, on request, from the corresponding author.